

Low- x physics and W and Z production at the LHC

A. M. Cooper-Sarkar¹

¹Particle Physics, Oxford University, Denys Wilkinson Building, Keble Rd, OXFORD, OX1 3RH, UK

1. INTRODUCTION

The kinematic plane for LHC is shown in Fig. 1, which translates the kinematics for producing a state of mass M and rapidity y into the deep inelastic scattering variables, Q^2 , the scale of the hard sub-process, and the Bjorken x values of the participating partons. The scale of the process is given by $Q^2 = M^2$ and the Bjorken x values by, $x_1 = (M/\sqrt{s})\exp(y)$, and, $x_2 = (M/\sqrt{s})\exp(-y)$, where y is the parton rapidity, $y = \frac{1}{2}\ln\frac{(E+pl)}{(E-pl)}$. Thus, at central rapidity, these x values are equal, but as one moves away from central rapidity, one parton moves to higher x and one to lower x , as illustrated by the lines of constant y on the plot. The first physics to be studied at the LHC will be at relatively low scales, where the large cross-sections ensure that even low luminosity running will yield copious numbers of events. Thus the LHC will begin by studying standard model (SM) physics, calibrating our knowledge of the detectors on these well known processes. Study of Fig. 1 makes it clear that the cross-sections for these processes are only well known if the parton distribution functions (PDFs) of the proton are well known at small- x . This assumes that the theoretical formalism of NLOQCD, as embodied in the DGLAP equations, is valid at small- x , since this is the formalism used for determining PDFs. In the present contribution we address the question of how PDF uncertainties at low x affect the SM processes of W and Z production at the LHC.

The major source of information on low- x physics in the last decade has been the HERA data. One of the most striking results of HERA was observation of an unexpected rise of the F_2 structure function at low- x . The interpretation of the rise in F_2 , in the DGLAP formalism, attributes it to a strong rise in the gluon distribution function at low- x , since the gluon drives the sea distributions by $g \rightarrow q\bar{q}$ splitting. In fact, the DGLAP equations predict that, at high Q^2 ($\gtrsim 100\text{GeV}^2$), a steep rise of the gluon and the sea at low- x will evolve from flat input shapes at a low Q^2 ($\sim 4\text{GeV}^2$). Nevertheless the rise was unexpected, firstly, because most theoreticians expected any such tendency to be tamed either by screening effects, or by gluon recombination at high gluon density. Secondly, because the rise was already present for low Q^2 ($\sim 1 - 2\text{GeV}^2$) - even lower than the conventional starting scale for QCD evolution. Hence the observation of the rise led to excitement in a somewhat orthogonal section of the theoretical community, where a steep rise at low Q^2 had been predicted in the BFKL formalism, which resums diagrams involving $\ln(1/x)$. Such resummations are not part of the conventional DGLAP $\ln(Q^2)$ summations.

However, even though the observation of a rise of F_2 at low x and low Q^2 defied conventional prejudice, it can be accommodated within the conventional DGLAP formalism provided sufficiently flexible input shapes are used at a low enough input scale (now taken to be $Q^2 \sim 1\text{GeV}^2$). In fact it turns out that whereas the input sea distribution is still rising at low- x , the input gluon distribution has turned over to become valence-like, and is even allowed to become negative in some parametrisations. Fig. 2 illustrates this behaviour in the sea and gluon PDFs, together with the data used to extract them. This counter intuitive behaviour has led many QCD theorists to believe that the conventional formalism is in need of extension [1]. The contribution of R. Ball to these proceedings describes modern work in this area. The present contribution is concerned with how well the PDFs are known at low- x , within the conventional framework, and how this affects the predictions for W and Z production at the LHC. These processes have been suggested as ‘standard-candles’ for the measurement of luminosity because their cross-sections are ‘well known’. In the present contribution we investigate to what extent this is really true- and what might be done about it.

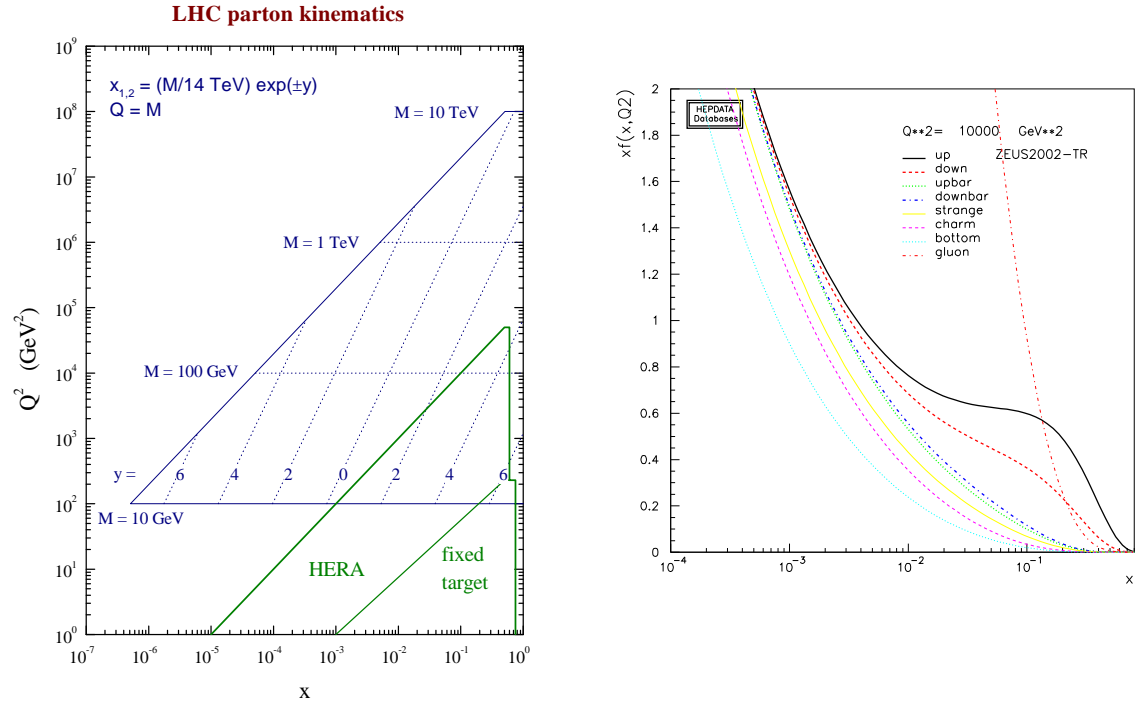


Fig. 1: Left plot: The LHC kinematic plane (thanks to James Stirling). Right plot: PDF distributions at $Q^2 = 10,000 \text{ GeV}^2$.

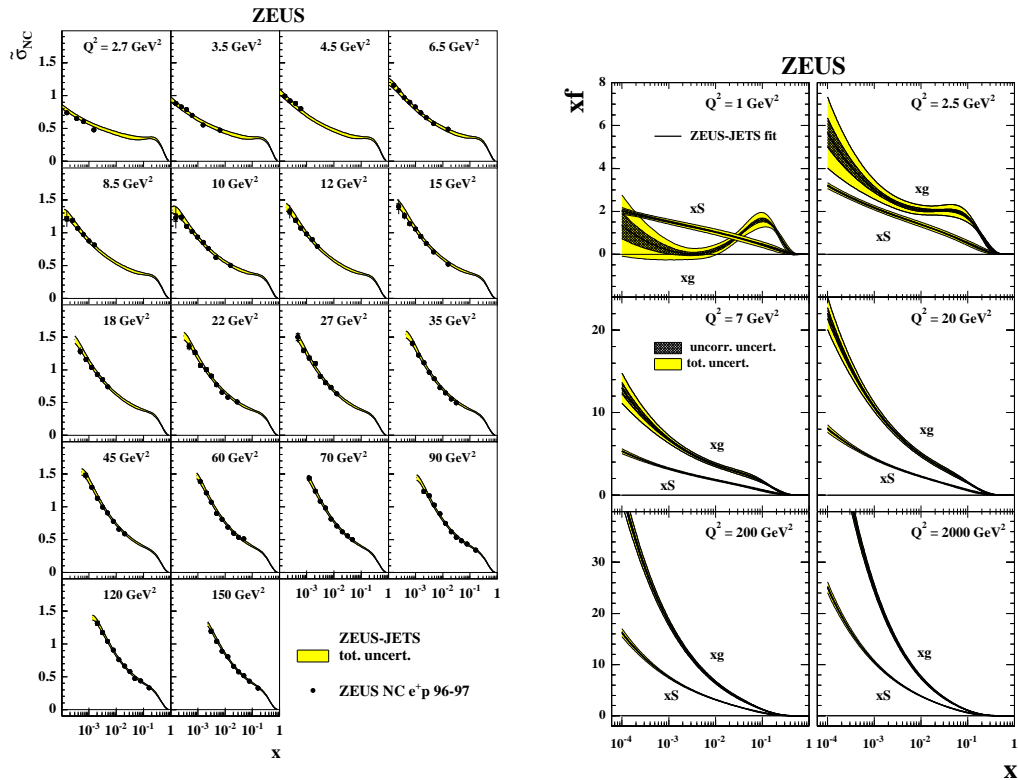


Fig. 2: Left side: ZEUS data on F_2 showing the rise at low x , for various Q^2 . Right side: the gluon and sea PDFs extracted from these data in the ZEUSJETS PDF fit, for various Q^2 , illustrating the turnover of the gluon PDF at low Q^2 .

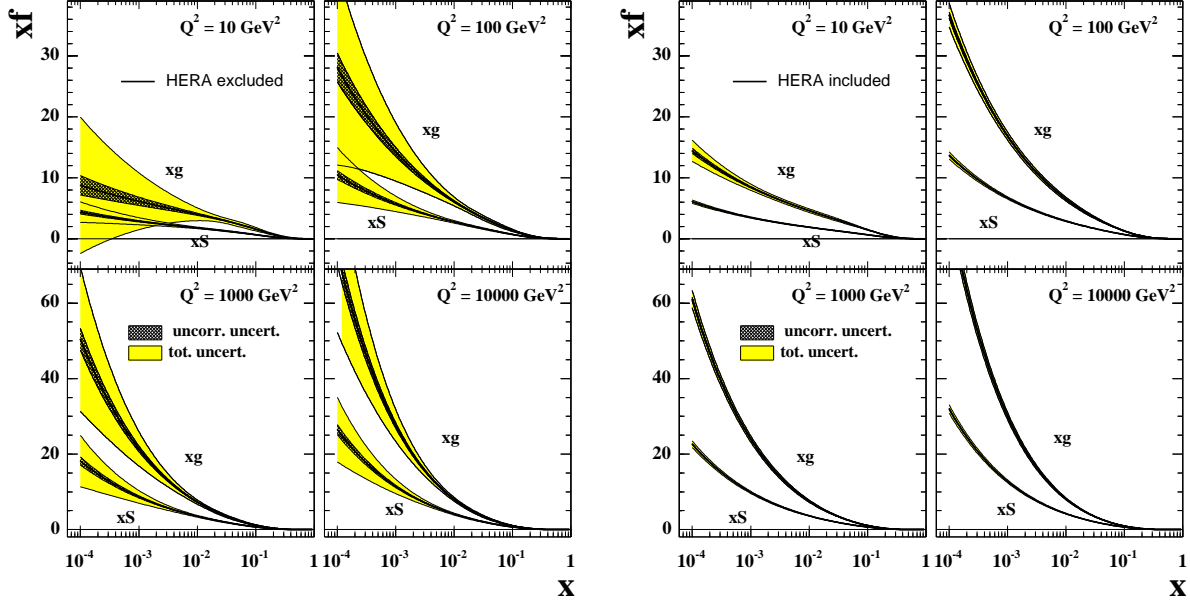


Fig. 3: Sea (xS) and gluon (xg) PDFs, as a function of x , for various Q^2 values: left plot; from the ZEUS-S global PDF analysis not including HERA data; right plot: from the ZEUS-S global PDF analysis including HERA data

2. W AND Z PRODUCTION AT THE LHC

At leading order (LO), W and Z production occur by the process, $q\bar{q} \rightarrow W/Z$. Consulting Fig. 1, we see that at central rapidity, the participating partons have small momentum fractions, $x \sim 0.005$, and over the measurable rapidity range, $|y| < 2.4$, x values remain in the range, $5 \cdot 10^{-4} < x < 0.05$. Thus, in contrast to the situation at the Tevatron, the scattering is happening dominantly between sea quarks and antiquarks. Furthermore, the high scale of the process $Q^2 = M^2 \sim 10,000 \text{ GeV}^2$ ensures that the gluon is the dominant parton as also illustrated in Fig. 1, where the PDFs for all parton flavours are shown for $Q^2 \sim 10,000 \text{ GeV}^2$. Hence the sea quarks have mostly been generated by the flavour blind $g \rightarrow q\bar{q}$ splitting process. Thus the precision of our knowledge of W and Z cross-sections at the LHC is crucially dependent on the uncertainty on the momentum distribution of the gluon at low- x . This is where the HERA data come in.

Fig. 3 shows the sea and gluon PDFs (and their uncertainties) extracted from an NLO QCD PDF fit analysis to world data on deep inelastic scattering, before and after HERA data are included. The latter fit is the ZEUS-S global fit [2], whereas the former is a fit using the same fitting analysis but leaving out the ZEUS data. The full PDF uncertainties for both fits are calculated from the eigenvector PDF sets of the ZEUS-S analysis using LHAPDF [3]. The improvement in the level of uncertainty is striking.

Fig. 4 illustrates how this improved knowledge of the gluon and sea distributions has improved our knowledge of W and Z cross-sections. It shows W and Z rapidity spectra predicted using the PDFs extracted from the global PDF fit which does not include the HERA data, compared to those extracted from the similar global PDF fit which does include HERA data. The corresponding predictions for the W/Z cross-sections, decaying to the lepton decay mode, are summarised in Table 1. The uncertainties in the predictions for these cross-sections have decreased from $\sim 16\%$ pre-HERA to $\sim 3.5\%$ post-HERA. There could clearly have been no talk of using these processes as standard candle processes, without the HERA data.

The post-HERA level of precision illustrated in Fig. 4 is taken for granted in modern analyses. However, when considering the PDF uncertainties on the Standard Model (SM) predictions it is necessary

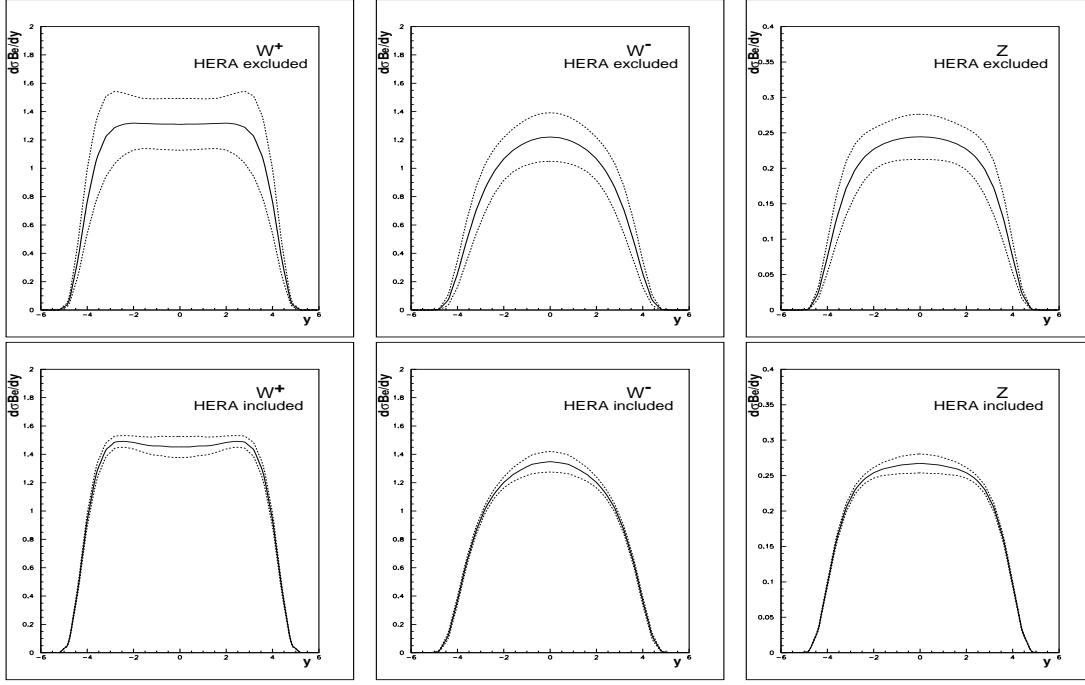


Fig. 4: LHC W^+ , W^- , Z rapidity distributions and their PDF uncertainties: Top Row: from the ZEUS-S global PDF analysis not including HERA data; left plot W^+ ; middle plot W^- ; right plot Z ; Bottom Row: from the ZEUS-S global PDF analysis including HERA data; left plot W^+ ; middle plot W^- ; right plot Z

PDF Set	$\sigma(W^+).B(W^+ \rightarrow l^+\nu_l)$	$\sigma(W^-).B(W^- \rightarrow l^-\bar{\nu}_l)$	$\sigma(Z).B(Z \rightarrow l^+l^-)$
ZEUS-S no HERA	10.63 ± 1.73 nb	7.80 ± 1.18 nb	1.69 ± 0.23 nb
ZEUS-S	12.07 ± 0.41 nb	8.76 ± 0.30 nb	1.89 ± 0.06 nb
CTEQ6.1	11.66 ± 0.56 nb	8.58 ± 0.43 nb	1.92 ± 0.08 nb
MRST01	11.72 ± 0.23 nb	8.72 ± 0.16 nb	1.96 ± 0.03 nb

Table 1: LHC W/Z cross-sections for decay via the lepton mode, for various PDFs

not only to consider the uncertainties of a particular PDF analysis, but also to compare PDF analyses. Fig. 5 compares the predictions for W^+ production for the ZEUS-S PDFs with those of the CTEQ6.1 [4] PDFs and the MRST01 [5] PDFs¹. The corresponding W^+ cross-sections, for decay to leptonic mode are given in Table 1. Comparing the uncertainty at central rapidity, rather than the total cross-section, we see that the uncertainty estimates are somewhat larger: $\sim 6\%$ for ZEUS-S; $\sim 8\%$ for CTEQ6.1M and $\sim 3\%$ for MRST01. The difference in the central value between ZEUS-S and CTEQ6.1 is $\sim 4\%$. Thus the spread in the predictions of the different PDF sets is comparable to the uncertainty estimated by the individual analyses. Since the measurable rapidity range is restricted to central rapidity it is more prudent to use these uncertainty estimates when considering if W, Z cross-sections can be used as luminosity monitors. Comparing the results from the three PDF extractions it seems reasonable to use generous estimate of the CTEQ6.1 analysis, 8%, as an estimate of how well the luminosity could be measured, at the present level of uncertainty. We subject this estimate to some further reality checks below and in Sec. 3. and we discuss the possibility of improving this estimate with early LHC data in Sec. 4.

Since the PDF uncertainty feeding into the W^+ , W^- and Z production is mostly coming from the gluon PDF, for all three processes, there is a correlation in their uncertainties, which can be removed by

¹MRST01 PDFs are used because the full error analysis is available for this PDF set.

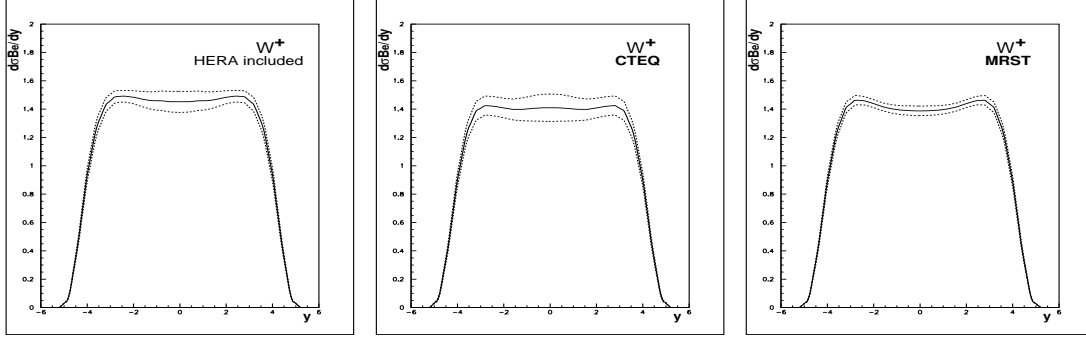


Fig. 5: LHC W^+ rapidity distributions and their PDF uncertainties: left plot, ZEUS-S PDFs; middle plot, CTEQ6.1 PDFs; right plot: MRST01 PDFs.

taking ratios. The upper half of Fig. 6 shows the W asymmetry

$$A_W = (W^+ - W^-)/(W^+ + W^-).$$

for CTEQ6.1 PDFs. The PDF uncertainties on the asymmetry at central rapidity are about 5%, smaller than those on the W spectra themselves, and a PDF eigenvector decomposition indicates that sensitivity to u and d quark flavour distributions is now evident. Even this residual flavour sensitivity can be removed by taking the ratio

$$A_{ZW} = Z/(W^+ + W^-)$$

as also shown in Fig. 6. This quantity is almost independent of PDF uncertainties, which are now as small as 0.5%, within the CTEQ6.1 PDF analysis.

However, as before, it is necessary to compare these quantities between different PDF analyses. The variation in the predictions for the ratio A_{ZW} between PDF analyses (MRST01, ZEUS-S and Alekhin02 PDFs have been compared to CTEQ6.1) is outside the PDF uncertainty estimates of the different analyses, but it is still only $\sim 5\%$. Hence this ratio could be used as an SM benchmark measurement. The ratio, A_W , shows a much more striking difference between MRST01 PDFs and the others. This is illustrated in the lower half of Fig. 6 for the ZEUS-S, CTEQ6.1 and MRST01 PDFs, in the measurable rapidity range. There is a difference of $\sim 25\%$ in the predictions. The origin of this difference between MRST and other PDFs is in the valence spectra. At leading order, the dominant contribution to A_W is

$$A_W = \frac{u\bar{d} - d\bar{u}}{u\bar{d} + d\bar{u}}. \quad (1)$$

At central rapidity, $x \sim 0.005$, for both partons and consequently $\bar{u} \approx \bar{d}^2$. Thus

$$A_W = \frac{u - d}{u + d} = \frac{u_v - d_v}{u_v + d_v + 2\bar{q}} \quad (2)$$

and A_W depends on the difference of the valence quarks. The quantity $u_v - d_v$, is different for MRST and CTEQ, and this difference is outside the PDF uncertainty estimates of either analysis. However, these uncertainty estimates are themselves unreliable for valence spectra at $x \sim 0.005$, since there is no data on valence quantities at such small x . The LHC can provide the first such measurement.

To assess if LHC measurements will actually be discriminating we must first account for the fact that W 's decay, and are most easily detected from their leptonic decays. Thus we actually measure the decay lepton rapidity spectra rather than the W rapidity spectra. The upper half of Fig. 7 shows

²Even if some fairly wild assumptions as to the shape of $\bar{d} - \bar{u}$ are made for low Q^2 , the absolute size of \bar{q} evolves with Q^2 to become very large at $Q^2 = M_W^2$, whereas the difference does not evolve, and becomes relatively small.

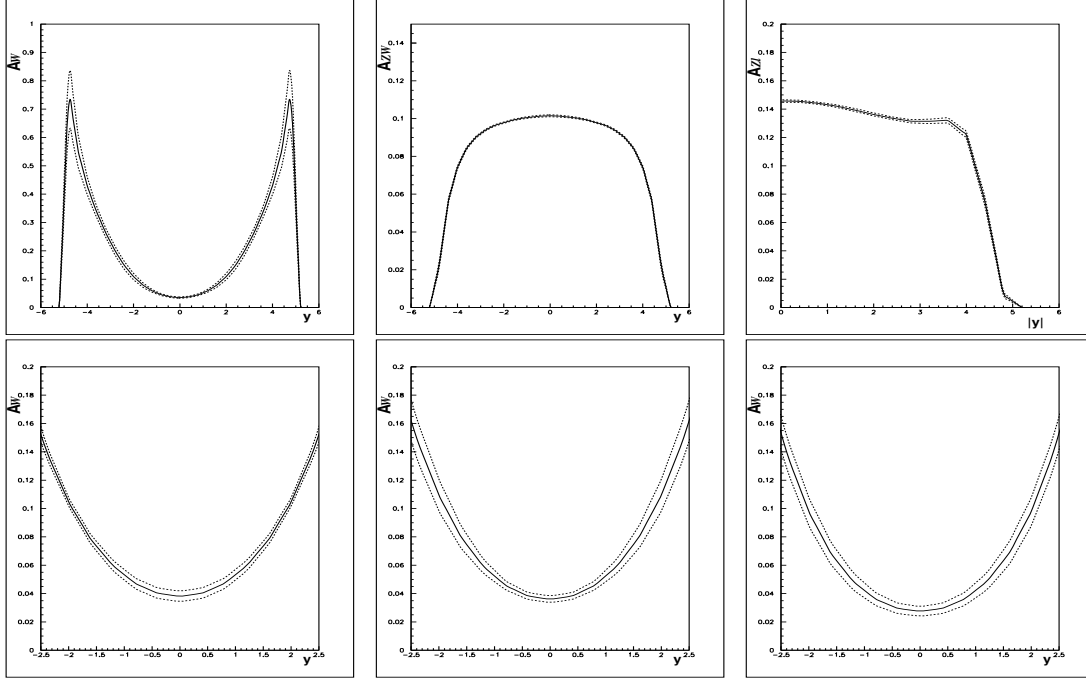


Fig. 6: Top row: predictions from the CTEQ6.1 PDFs: left plot, the W asymmetry, A_W ; middle plot, the ratio, A_{ZW} ; right plot, the ratio, A_{Zl} . Bottom row: the W asymmetry, A_W , within the measurable rapidity range, as predicted using different PDF analyses; left plot ZEUS-S; middle plot CTEQ6.1; right plot MRST01.

these rapidity spectra for positive and negative leptons from W^+ and W^- decay together with the lepton asymmetry,

$$A_l = (l^+ - l^-)/(l^+ + l^-)$$

for the CTEQ6.1 PDFs. A cut of, $p_t > 25\text{GeV}$, has been applied on the decay lepton, since it will not be possible to identify leptons with small p_t . A particular lepton rapidity can be fed from a range of W rapidities so that the contributions of partons at different x values are smeared out in the lepton spectra. Nevertheless the broad features of the W spectra and the sensitivity to the gluon parameters are reflected in the lepton spectra, resulting in a similar estimate ($\sim 8\%$) of PDF uncertainty at central rapidity for the CTEQ6.1 PDFs. The lepton asymmetry shows the change of sign at large y which is characteristic of the $V - A$ structure of the lepton decay. The cancellation of the uncertainties due to the gluon PDF is not so perfect in the lepton asymmetry as in the W asymmetry. Even so, in the measurable rapidity range, the PDF uncertainty in the asymmetry is smaller than in the lepton spectra, being $\sim 5\%$, for the CTEQ6.1 PDFs. The Z to W ratio A_{ZW} has also been recalculated as a Z to leptons ratio,

$$A_{Zl} = Z/(l^+ + l^-)$$

illustrated in Fig. 6. Just as for A_{ZW} , the overall uncertainty in A_{Zl} is very small ($\sim 0.5\%$) for CTEQ6.1 PDFs.

It is again necessary to consider the difference between different PDF analyses for the predictions of the lepton spectra, A_{Zl} and A_l . For the lepton spectra, the spread in the predictions of the different PDF analyses of MRST01, CTEQ6.1 and ZEUS-S is comparable to the uncertainty estimated by the individual analyses, just as for the W spectra, and this is shown later in Fig. 8. Just as for A_{ZW} , there are greater differences in the predictions for A_{Zl} between PDF analyses than within any PDF analysis, but these differences remain within $\sim 5\%$ preserving this quantity as an SM benchmark measurement. Thus our previous estimate of the usefulness of these processes as luminosity monitors and SM benchmarks survives the reality check of the fact that we will measure the leptons, not the W 's.

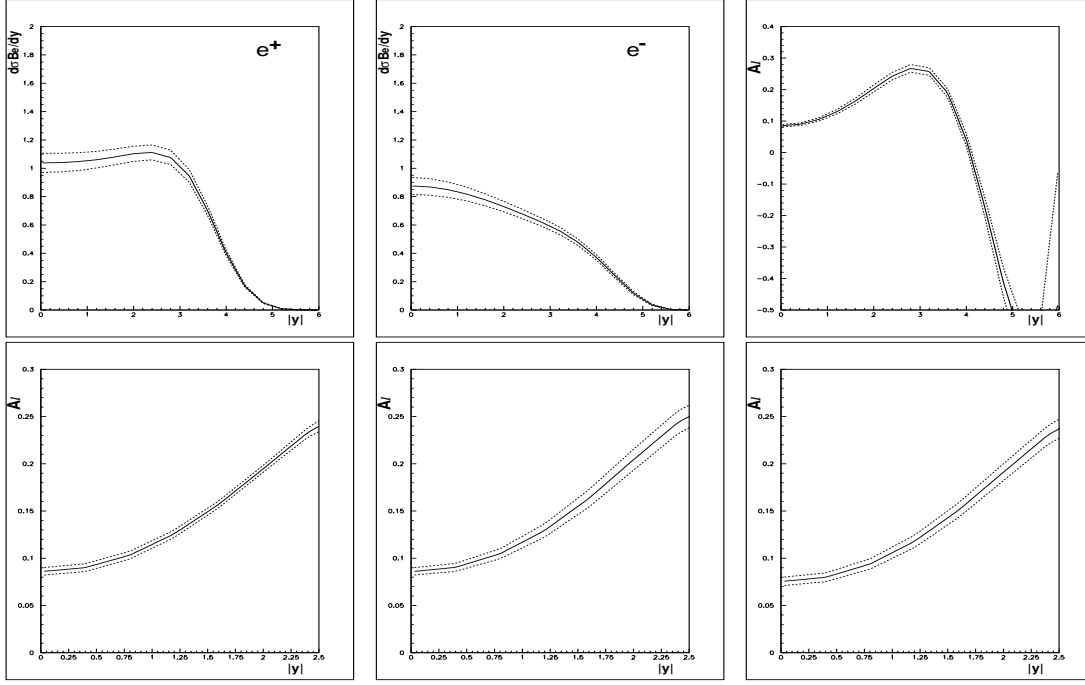


Fig. 7: Top row: lepton spectra from the CTEQ6.1 PDFs; left plot, decay e^+ rapidity spectrum; middle plot, decay e^- rapidity spectrum; right plot, lepton asymmetry, A_l . Bottom Row: the lepton asymmetry, A_l , from different PDF analyses; left plot ZEUS-S; middle plot CTEQ6.1; right plot MRST01

The significant differences which we noticed between the predictions of the different PDF analyses for A_W , remain in the predictions for A_l . The lower half of Fig. 7 compares these predictions for the ZEUS-S PDFs with those of the CTEQ6.1 PDFs and the MRST01 PDFs, in the measurable rapidity range. The discrepancy of $\sim 25\%$ which was found in A_W has been somewhat diluted to $\sim 15\%$ in A_l , but this should still be large enough for LHC measurements to discriminate, and hence to give information on the low- x valence distributions.

3. HOW WELL CAN WE ACTUALLY MEASURE W SPECTRA AT THE LHC?

The remainder of this contribution will be concerned with the question: how accurately can we measure the lepton rapidity spectra and can we use the early LHC data to improve on the current level of uncertainty?

We have simulated one million signal, $W \rightarrow e\nu_e$, events for each of the PDF sets CTEQ6.1, MRST2001 and ZEUS-S using HERWIG (6.505). For each of these PDF sets the eigenvector error PDF sets have been simulated by PDF reweighting and k-factors have been applied to approximate an NLO generation. A study has been made of the validity of both PDF reweighting and k-factor reweighting and this is reported in ref. [6]. The conclusion is that PDF reweighting is valid for reweighting the rapidity spectra when the PDF sets are broadly similar, as they are within any one PDF analysis. The k-factor reweighting to simulate NLO is also valid for the rapidity spectra for which it was designed.

The top part of Fig. 8, shows the e^\pm and A_l spectra at the generator level, for all of the PDF sets superimposed. As mentioned before, it is clear that the lepton spectra as predicted by the different PDF analyses are compatible, within the PDF uncertainties of the analyses. The events are then passed through the ATLFast fast simulation of the ATLAS detector. This applies loose kinematic cuts: $|\eta| < 2.5$, $p_{te} > 5\text{GeV}$, and electron isolation criteria. It also smears the 4-momenta of the leptons to mimic momentum dependent detector resolution. We then apply further cuts designed to eliminate the background preferentially. These criteria are:

- pseudorapidity, $|\eta| < 2.4$, to avoid bias at the edge of the measurable rapidity range
- $p_{te} > 25\text{GeV}$, high p_t is necessary for efficient electron identification

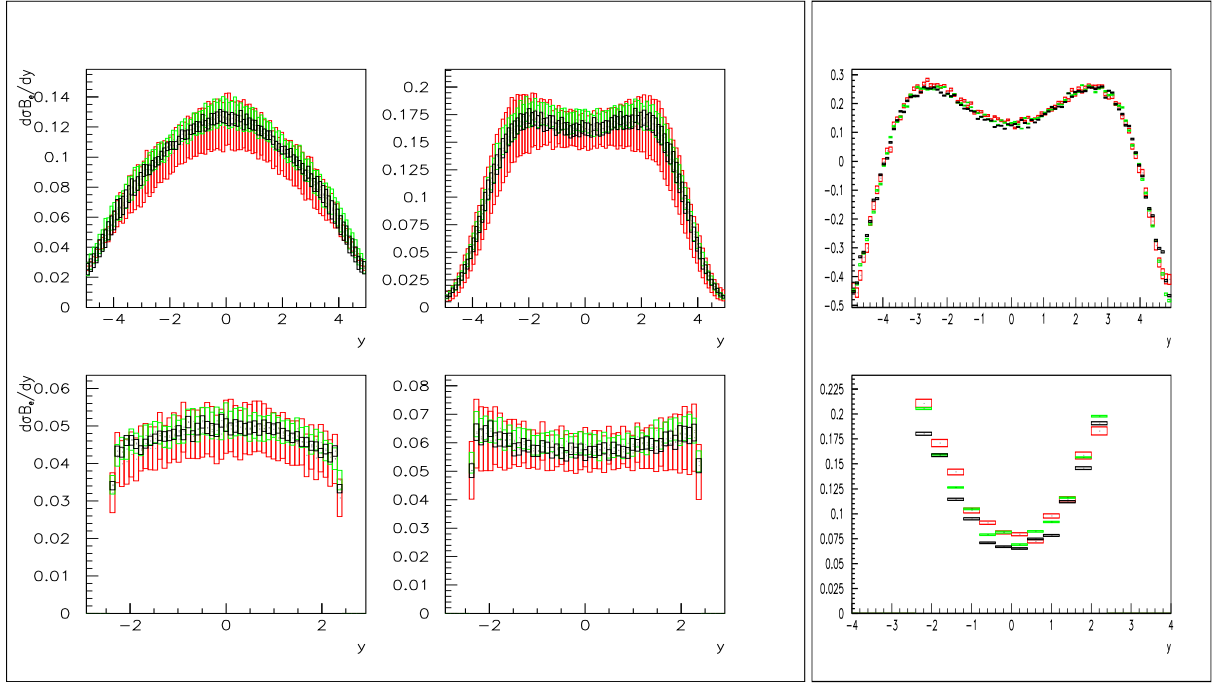


Fig. 8: Top row: e^- , e^+ and A_e rapidity spectra for the lepton from the W decay, generated using HERWIG + k factors and CTE6.1 (red), ZEUS-S (green) and MRST2001 (black) PDF sets with full uncertainties. Bottom row: the same spectra after passing through the ATLFast detector simulation and selection cuts.

- missing $E_t > 25$ GeV, the ν_e in a signal event will have a correspondingly large missing E_t
- no reconstructed jets in the event with $p_t > 30$ GeV, to discriminate against QCD background
- recoil on the transverse plane $p_t^{recoil} < 20$ GeV, to discriminate against QCD background

These cuts ensure that background from the processes: $W \rightarrow \tau \nu_\tau$; $Z \rightarrow \tau^+ \tau^-$; and $Z \rightarrow e^+ e^-$, is negligible ($\lesssim 1\%$) [6]. Furthermore, a study of charge misidentification has established that the lepton asymmetry will need only very small corrections ($\lesssim 0.5\%$), within the measurable rapidity range [6].

The lower half of Fig. 8, shows the e^\pm and A_l spectra at the detector level after application of these cuts, for all of the PDF sets superimposed. The level of precision of each PDF set, seen in the analytic calculations of Fig. 5, appears somewhat degraded at detector level, so that a net level of PDF uncertainty in the lepton spectra of $\sim 10\%$ is expected at central rapidity. Thus the usefulness of these processes as a luminosity monitor is somewhat compromised if a measurement to better than 10% is required.

The anticipated cancellation of PDF uncertainties in the asymmetry spectrum is observed, within each PDF set, such that the uncertainties predicted by each PDF set are $\sim 5\%$, but the spread between the MRST and CTEQ/ZEUS-S PDF sets is as large as $\sim 15\%$. Thus measurements which are accurate to about $\sim 5\%$ could provide useful information on the valence distributions at low x .

4. USING LHC DATA TO IMPROVE PRECISION ON PDFs

We now consider the possibility of improving on the current level of PDF uncertainty by using LHC data itself. The high cross-sections for W production at the LHC ensure that it will be the experimental systematic errors, rather than the statistical errors, which are determining. Our experience with the detector simulation leads us to believe that a systematic precision of $\sim 5\%$ could be achievable. We have optimistically imposed a random 4% scatter on our samples of one million W events, generated using different PDFs, in order to investigate if measurements at this level of precision will improve PDF uncertainties at central rapidity significantly, if they are input to a global PDF fit.

The upper left hand plot of Fig. 9 shows the e^+ rapidity spectra for events generated from the ZEUS-S PDFs compared to the analytic predictions for these same ZEUS-S PDFs. The lower left hand

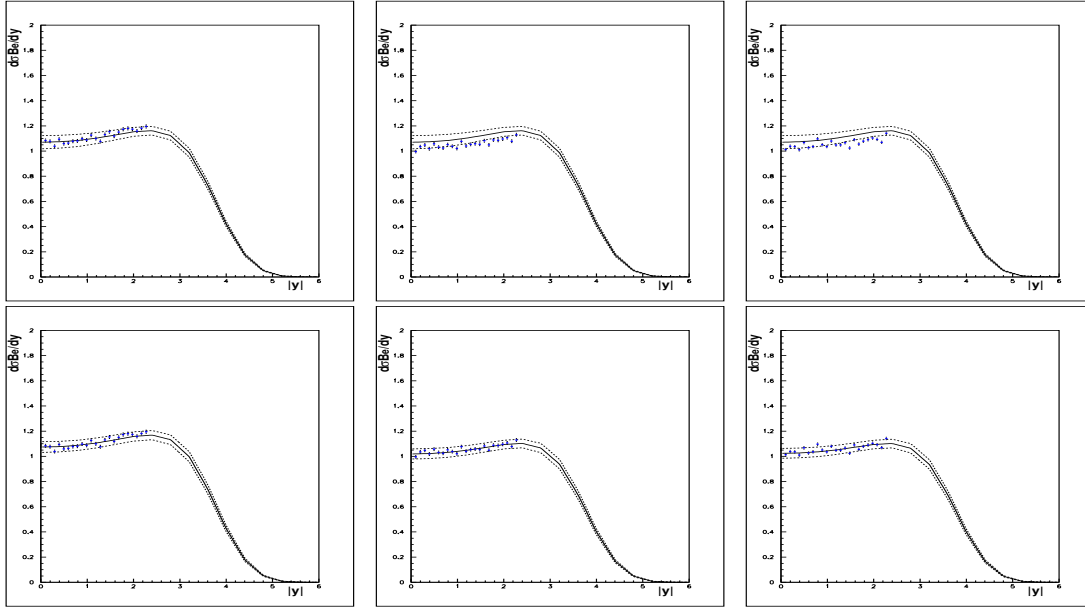


Fig. 9: Top row: e^+ rapidity spectra generated from: left plot, ZEUS-S PDFs; middle plot, CTEQ6.1 PDFs; right plot, CTEQ6.1 PDFs which have been passed through the ATLFast detector simulation and corrected back to generator level using ZEUS-S PDFs; compared to the analytic prediction using ZEUS-S PDFs. Bottom row: the same lepton rapidity spectra as above compared to the analytic prediction AFTER including these lepton pseudo-data in the ZEUS-S PDF fit.

plot illustrates the result if these events are then included in the ZEUS-S PDF fit (together with the e^- spectra which are not illustrated). The size of the PDF uncertainties, at $y = 0$, decreases from 6% to 4.5%. The largest improvement is in the PDF parameter λ_g controlling the low- x gluon at the input scale, Q_0^2 : $xg(x) \sim x^{\lambda_g}$ at low- x , $\lambda_g = -0.199 \pm 0.046$, before the input of the LHC pseudo-data, compared to, $\lambda_g = -0.196 \pm 0.029$, after input. Note that whereas the relative normalisations of the e^+ and e^- spectra are set by the PDFs, the absolute normalisation of the data is free in the fit so that no assumptions are made on our ability to measure luminosity. Secondly, we repeat this procedure for events generated using the CTEQ6.1 PDFs. This is illustrated in the middle section of Fig. 9. Before they are input to the fit, the cross-section for these events is on the lower edge of the uncertainty band of the ZEUS-S predictions (upper middle plot). If these events are then input to the fit the central value shifts and the uncertainty decreases (lower middle plot). The value of the parameter λ_g becomes, $\lambda_g = -0.189 \pm 0.029$, after input of these pseudo-data. Finally, to simulate the situation which really faces experimentalists, we generate events with CTEQ6.1, and pass them through the ATLFast detector simulation and cuts. We then correct back from detector level to generator level using a different PDF set- in this cases the ZEUS-S PDFs- since in practice we will not know the true PDFs. The upper right hand plot of Fig. 9 shows that the resulting corrected data look pleasingly like CTEQ6.1, but they are more smeared. When these data are input to the PDF fit the central values shift and errors decrease (lower right plot) just as for the perfect CTEQ6.1 pseudodata. The value of λ_g becomes, $\lambda = -0.181 \pm 0.030$, after input of these pseudodata. Thus we see that the bias introduced by the correction procedure from detector to generator level is small compared to the PDF uncertainty, and that measurements at the $\sim 4\%$ level should be able to improve the level of uncertainty of the PDF predictions.

CONCLUSIONS

We have investigated the PDF uncertainty on the predictions for W and Z production at the LHC, using the electron decay channel for the W s and taking into account realistic expectations for measurement accuracy and the cuts on data which will be needed to identify signal events from background processes. We conclude that, at the present level of PDF uncertainty, the decay lepton spectra can be used as a luminosity monitor but it is only good to $\sim 10\%$. However, we have also investigated the measurement accuracy necessary for early measurements of these decay lepton spectra to be useful in further

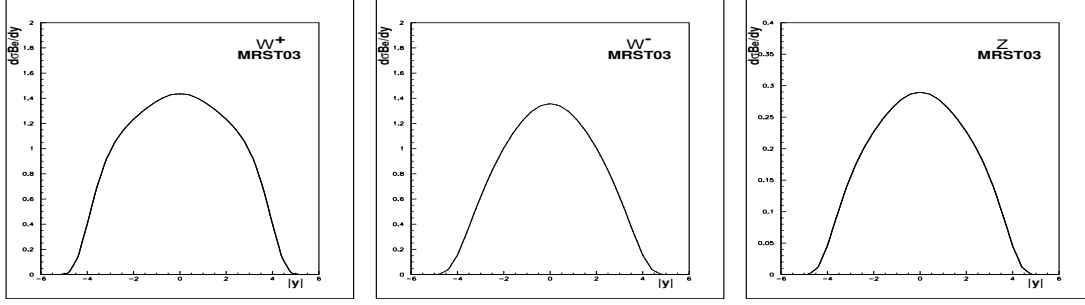


Fig. 10: LHC W^+ , W^- , Z rapidity distributions for the MRST03 PDFs: left plot W^+ ; middle plot W^- ; right plot Z

constraining the PDFs. A systematic measurement error of $\sim 4\%$ could provide useful extra constraints.

The ratio of Z to $W^+ + W^-$ production (measured via the lepton spectra) can provide an SM measurement which is relatively insensitive to PDF uncertainties. By contrast a measurement of the lepton asymmetry can provide the first measurements of the valence difference $u_v - d_v$ at small x .

We now return to the caveat made in the introduction: the current study has been performed using standard PDF sets which are extracted using NLO QCD in the DGLAP formalism. The extension to NNLO is straightforward, giving small corrections $\sim 1\%$. PDF analyses at NNLO including full accounting of the PDF uncertainties are not extensively available yet, so this small correction has not been pursued here. However, there may be much larger uncertainties in the theoretical calculations because the kinematic region involves low- x . The MRST group recently produced a PDF set, MRST03, which does not include any data for $x < 5 \times 10^{-3}$, in order to avoid the inappropriate use of the DGLAP formalism at small- x . Thus the MRST03 PDF set should only be used for $x > 5 \times 10^{-3}$. What is needed is an alternative theoretical formalism for smaller x , as suggested by R. Ball in these proceedings. It is clear that the use of this formalism would bring greater changes than the small corrections involved in going to NNLO. There may even be a need for more radical extensions of the theory at low- x due to high density effects.

The MRST03 PDF set may be used as a toy PDF set, to illustrate the effect of using very different PDF sets on our predictions. A comparison of Fig. 10 with Fig. 4 or Fig. 5 shows how different the analytic predictions are from the conventional ones, and thus illustrates where we might expect to see differences due to the need for an alternative formalism at small- x . Whereas these results may seem far fetched we should remind ourselves that moving into a different kinematic regime can provide surprises—as it did with the HERA data itself!

References

- [1] R. C. E. Devenish and A. M. Cooper-Sarkar, *Deep Inelastic Scattering Chap.9*. Oxford University Press, 2004.
- [2] S. ZEUS Coll., Chekanov, *Phys. Rev. D* **67** (2003) 012007.
- [3] M. Whalley, *Eur. Phys. J C* **23** (2002) 73.
- [4] J. Pumplin, *JHEP* **0207** (2002) 012.
- [5] A. D. Martin, *Eur. Phys. J C* **23** (2002) 73.
- [6] A. M. Tricoli, A. Cooper-Sarkar and G. Gwenlan, *hep-ex* **0509002** (2005).

